The Astrophysical Journal, 881:167 (4pp), 2019 August 20 https://doi.org/10.3847/1538-4357/ab364f

Erratum: "Quantifying Feedback from Narrow Line Region Outflows in Nearby Active Galaxies. II. Spatially Resolved Mass Outflow Rates for the QSO2 Markarian 34" (2018, ApJ, 867, 88)*†

M. Revalski[1,8], D. Dashtamirova[1], D. M. Crenshaw[1], S. B. Kraemer[2], T. C. Fischer[3,9], H. R. Schmitt[4], C. L. Gnilka[1], J. Schmidt[10], M. Elvis[5], G. Fabbiano[5], T. Storchi-Bergmann[5,6], W. P. Maksym[5], and P. Gandhi[7]
[1] Department of Physics and Astronomy, Georgia State University, 25 Park Place, Suite 605, Atlanta, GA 30303, USA; revalski@astro.gsu.edu
[2] Institute for Astrophysics and Computational Sciences, Department of Physics, The Catholic University of America, Washington, DC 20064, USA
[3] Astrophysics Science Division, Goddard Space Flight Center, Code 665, Greenbelt, MD 20771, USA
[4] Naval Research Laboratory, Washington, DC 20375, USA
[5] Harvard-Smithsonian Center for Astrophysics, 60 Garden St., Cambridge, MA 02138, USA
[6] Departamento de Astronomia, Universidade Federal do Rio Grande do Sul, IF, CP 15051, 91501-970 Porto Alegre, RS, Brazil
[7] Department of Physics and Astronomy, University of Southampton, Southampton SO17 3RT, UK
Received 2019 July 23; published 2019 August 23

In the published article, the ionized gas mass profile, mass outflow rates, and outflow energetics presented in Table 9 and Figures 9 and 10 were underestimated due to a calculation error (Revalski et al. 2018b). This arose from adopting a mean density law from our photoionization models where each component's density was weighted by its contribution to the luminosity rather than its contribution to the mass. This caused the average gas density at each location to be weighted toward higher values, corresponding to an underestimation of the gas mass at each radius. We have corrected this error by calculating the mass in each high-, medium-, and low-ionization component individually, and then summing their masses.

This erratum contains corrected values for the results presented in Table 9 and Figures 9 and 10 of the published article. The result of this correction is that the total ionized gas mass summed over all radii increases by a factor of ∼10, with the majority located at larger radii. This trend with radius is due to the fact that the photoionization models are dominated by a single medium ionization component at smaller radii ($R \lesssim 1$ kpc) such that the luminosity-weighted mean density is closer to the mass-weighted mean density at those locations.

The total ionized gas mass contained within the APO long-slit observations that we used to construct our photoionization models is $M \approx 3.2 \times 10^8\,M_\odot$, which may be confirmed using the values provided in Tables 6 and 7 in conjunction with Equation (8) in the published article. These models span a radial extent of $\pm 2\farcs2$ from the nucleus, while the *HST* kinematics allowed us to derive an outflow velocity law extending to $\pm 1\farcs5$. Inside of this radius, the correct ionized gas mass is $M \approx 3.3 \times 10^7\,M_\odot$. We determined that half of the material is outflowing, leading to an outflow gas mass of $M \approx 1.6 \times 10^7 M_\odot$. These values are a factor of ∼10 higher than those quoted in the published article.

The numerical values of several quantities listed in the abstract and throughout the discussion and conclusions require revision. The outflow contains a total ionized gas mass of $M \approx 1.6 \times 10^7\,M_\odot$. The peak mass outflow rate is $\dot{M}_{\rm out} \approx 12.5 \pm 2.4\,M_\odot\,{\rm yr}^{-1}$ at a distance of 470 pc from the nucleus, with a spatially integrated kinetic energy of $E \approx 1.0 \times 10^{56}$ erg. The central bin mass is $M \approx 2.1 \times 10^5 M_\odot$, with $M \approx 8.4 \times 10^4 M_\odot$ of that outflowing. The peak momentum flow rate is $\dot{p} \approx 1.5 \times 10^{35}$ dyne, which is ∼28% of the active galactic nucleus (AGN) photon momentum. The peak kinetic luminosity reaches ∼0.1%–0.3% of the bolometric luminosity, which is $\log(L_{\rm bol}) = 46.2 \pm 0.4\,{\rm erg\ s}^{-1}$.

In Section 7.2, using the [S II] line ratios to determine the gas density results in an NLR gas mass estimate that is ∼0.06–1.24 times the value from our models ($\sim 3.3 \times 10^7\,M_\odot$). In Section 8, the first conclusion point should be updated with the correct mass estimate of $M \approx 1.6 \times 10^7\,M_\odot$ and outflow kinetic energy of $E \approx 1.0 \times 10^{56}$ erg. The second conclusion point should be updated with the correct peak mass outflow rate of $\dot{M}_{\rm out} \approx 12.5 \pm 2.4\,M_\odot\,{\rm yr}^{-1}$, with the implication that the peak rate is no longer similar to the AGN in our previous studies (Crenshaw et al. 2015; Revalski et al. 2018a).

Overall, the discussion and conclusions in the published article are correct. While the total ionized gas mass is larger by a factor of ∼10 than originally reported, the majority of this gas is at larger radii than those displaying outflow kinematics. As noted above, the enclosed ionized gas mass at $R \leqslant 1\farcs5$ is $M \approx 3.3 \times 10^7\,M_\odot$, while extending out to $R \leqslant 2\farcs2$ encompasses $M \approx 3.2 \times 10^8\,M_\odot$. This indicates that there is an immense amount of ionized gas in the ENLR, which is important for future studies that compare the amount of mass in different gas phases. Finally, it is worthwhile to note that this issue did not affect our results for Mrk 573 (Revalski et al. 2018a), as that analysis did not require interpolation of the model densities.

* Based on observations made with the NASA/ESA *Hubble Space Telescope*, obtained from the Data Archive at the Space Telescope Science Institute, which is operated by the Association of Universities for Research in Astronomy, Inc., under NASA contract NAS 5-26555. These observations are associated with program # 14360.
† Based in part on observations obtained with the Apache Point Observatory 3.5 m telescope, which is owned and operated by the Astrophysical Research Consortium.
[8] National Science Foundation Graduate Research Fellow (DGE-1550139).
[9] James Webb Space Telescope NASA Postdoctoral Program Fellow.
[10] Designer/Developer for the Astrophysics Source Code Library.

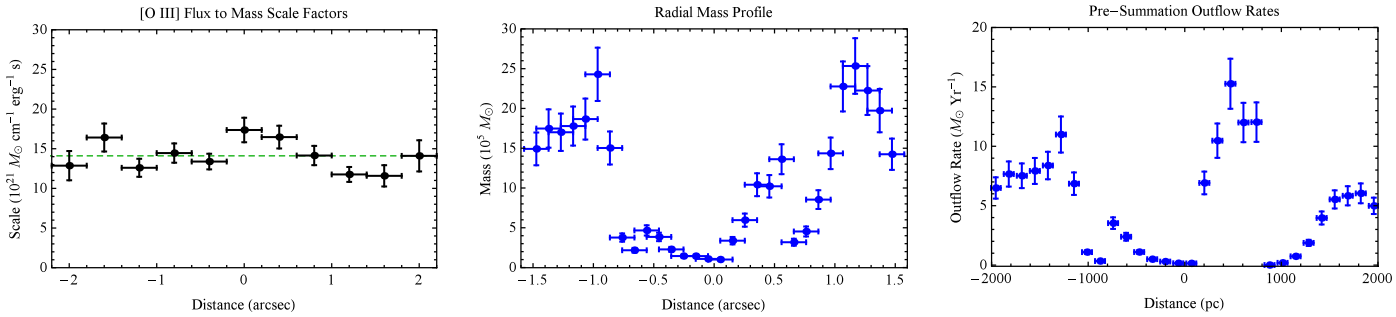

Figure 9. Corrected center and right panels for Figure 9. The center panel shows the ionized gas mass profile in units of $10^5 M_\odot$ calculated from the total flux in each semi-ellipse. The right panel shows the mass outflow rates assuming that all of the material is in outflow. Distances in arcseconds are the observed values, while distances in pc are corrected for projection.

Table 9
Radial Mass Outflow and Energetic Results

Distance (pc) (1)	Velocity (km s^{-1}) (2)	Mass (10^5 $M_\odot$) (3)	$\dot{M}$ ($M_\odot$ yr^{-1}) (4)	Energy (10^{53} erg) (5)	$\dot{E}$ (10^{41} erg s^{-1}) (6)	Momentum (10^{46} dyne s) (7)	$\dot{P}$ (10^{34} dyne) (8)
67.5	191.8	0.84 ± 0.12	0.12 ± 0.02	0.31 ± 0.06	0.03 ± 0.01	0.57 ± 0.11	0.01 ± 0.01
202.4	2347.9	2.26 ± 0.31	4.02 ± 0.78	140.31 ± 27.37	90.98 ± 17.75	11.14 ± 2.17	6.74 ± 1.31
337.4	1976.6	4.17 ± 0.57	6.24 ± 1.22	183.52 ± 35.80	101.63 ± 19.83	17.00 ± 3.32	8.81 ± 1.72
472.4	1789.2	9.18 ± 1.27	12.45 ± 2.43	307.48 ± 59.98	142.32 ± 27.76	34.25 ± 6.68	14.77 ± 2.88
607.3	1358.2	2.94 ± 0.41	3.03 ± 0.59	56.98 ± 11.11	24.33 ± 4.75	12.95 ± 2.53	2.74 ± 0.53
742.3	1108.4	2.51 ± 0.35	2.11 ± 0.41	30.77 ± 6.00	17.32 ± 3.38	13.07 ± 2.55	1.48 ± 0.29
877.2	46.0	1.15 ± 0.16	0.04 ± 0.01	0.10 ± 0.02	0.05 ± 0.01	0.90 ± 0.18	0.01 ± 0.01
1012.2	113.0	4.06 ± 0.56	0.35 ± 0.07	1.14 ± 0.22	0.50 ± 0.10	3.24 ± 0.63	0.05 ± 0.01
1147.1	368.6	13.20 ± 1.82	3.69 ± 0.72	25.63 ± 5.00	7.84 ± 1.53	19.41 ± 3.79	1.23 ± 0.24
1282.1	533.5	13.53 ± 1.87	5.47 ± 1.07	41.37 ± 8.07	12.37 ± 2.41	29.54 ± 5.76	1.99 ± 0.39
1417.0	350.7	23.01 ± 3.17	6.11 ± 1.19	34.82 ± 6.79	9.72 ± 1.90	29.01 ± 5.66	1.67 ± 0.33
1552.0	407.1	18.39 ± 2.54	5.67 ± 1.11	34.24 ± 6.68	9.27 ± 1.81	27.14 ± 5.29	1.64 ± 0.32
1687.0	440.4	16.17 ± 2.23	5.40 ± 1.05	33.36 ± 6.51	9.03 ± 1.76	26.43 ± 5.16	1.60 ± 0.31
1821.9	517.0	24.38 ± 3.36	9.55 ± 1.86	66.48 ± 12.97	9.45 ± 1.84	27.05 ± 5.28	3.19 ± 0.62
1956.9	538.7	19.68 ± 2.71	8.03 ± 1.57	57.31 ± 11.18	8.21 ± 1.60	22.76 ± 4.44	2.75 ± 0.54

Note. The corrected numerical results for the mass and energetic quantities as a function of radial distance for the outflowing gas component. Columns are (1) deprojected distance from the nucleus, (2) mass-weighted mean velocity, (3) gas mass in units of 10^5 $M_\odot$, (4) mass outflow rates, (5) kinetic energies, (6) kinetic energy outflow rates, (7) momenta, and (8) momenta flow rates. These results, shown in Figure 10, are the sum of the individual radial profiles calculated for each of the semi-annuli. The value at each distance is the quantity contained within the annulus of width δr.

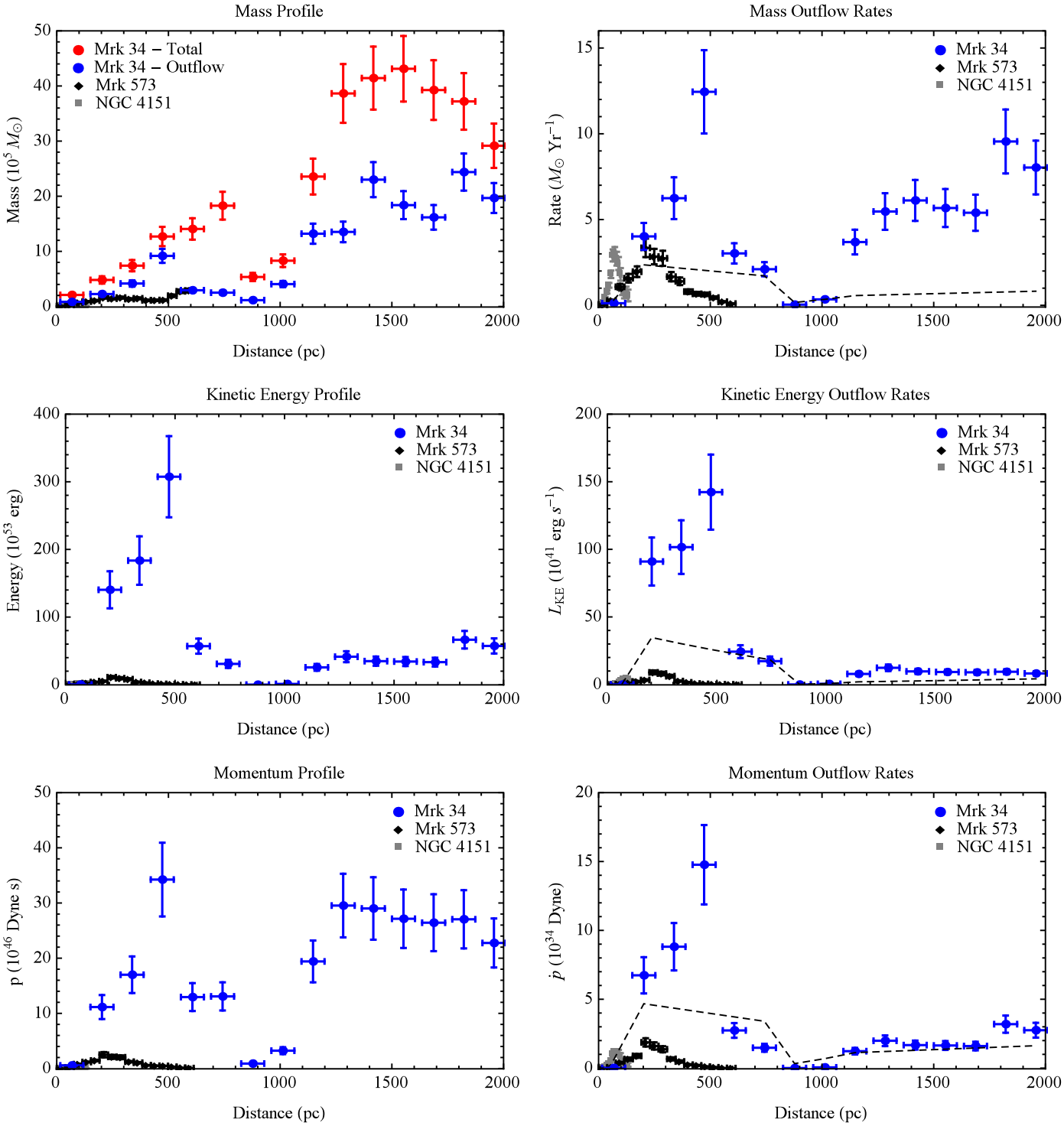

Figure 10. Corrected panels for Figure 10. Top left to bottom right are the azimuthally summed mass profiles, mass outflow rates, kinetic energy profiles, kinetic energy outflow rates, momentum profiles, and momentum outflow rates for Mrk 34, Mrk 573 (Revalski et al. 2018a), and NGC 4151 (Crenshaw et al. 2015). The red points represent the result that is obtained assuming that all of the mass is in outflow, and the blue points show the net result after multiplying by the fraction of flux in outflow as shown in Figure 4. The dashed lines represent the profiles that would result from the mass in the center bin ($M \approx 2.1 \times 10^5 M_\odot$) traveling through the velocity profile. Quantities are per bin, and targets have different bin sizes.

ORCID iDs

M. Revalski https://orcid.org/0000-0002-4917-7873
D. M. Crenshaw https://orcid.org/0000-0002-6465-3639
S. B. Kraemer https://orcid.org/0000-0002-6928-9848
T. C. Fischer https://orcid.org/0000-0002-3365-8875
H. R. Schmitt https://orcid.org/0000-0001-7376-8481
J. Schmidt https://orcid.org/0000-0002-2617-5517
M. Elvis https://orcid.org/0000-0001-5060-1398
G. Fabbiano https://orcid.org/0000-0002-3554-3318
T. Storchi-Bergmann https://orcid.org/0000-0003-1772-0023
W. P. Maksym https://orcid.org/0000-0002-2203-7889
P. Gandhi https://orcid.org/0000-0003-3105-2615

References

Crenshaw, D. M., Fischer, T. C., Kraemer, S. B., & Schmitt, H. R. 2015, ApJ, 799, 83
Revalski, M., Crenshaw, D. M., Kraemer, S. B., et al. 2018a, ApJ, 856, 46
Revalski, M., Dashtamirova, D., Crenshaw, D. M., et al. 2018b, ApJ, 867, 88